UNIVERSITY OF CALIFORNIA SAN DIEGO

Theoretical Modeling of the o-Cresolphthalein Complexone Assay for Bone Calcium Resorption

A thesis submitted in partial satisfaction of the requirements for the degree Master of Science

in

Bioengineering

by

Swetha Mohan

Committee in charge:

Professor Robert L. Sah, Chair
Professor Koichi Masuda
Professor Christian M. Metallo

2020

Copyright

Swetha Mohan, 2020

All rights reserved.

The thesis of Swetha Mohan is approved, and it is acceptable in quality and form for publication on microfilm and electronically:

Chair

University of California San Diego

2020

DEDICATION

I would like to dedicate this thesis to my parents, and friends from India and San Diego.

TABLE OF CONTENTS

LIST OF FIGURES

LIST OF TABLES

ACKNOWLEDGEMENTS

Firstly, I would like to acknowledge Dr. Robert L. Sah, for giving me an opportunity in his lab and providing continuous support and guidance throughout the project. I would also like to thank the other members of the lab who helped me get started in lab and helped me whenever in need. I would also like to acknowledge the constant support provided by my family and friends from overseas and around here. I'm very grateful for all the help as without them, this wouldn't have been possible.

The study described in Chapter 2 of this paper is being prepared for submission for publication. Swetha, Mohan; Sah, Robert L. "Theoretical Modeling of the o-Cresolphthalein Complexone Assay for Bone Calcium Resorption". The thesis author was the primary investigator and author of this material.

ABSTRACT OF THE THESIS

Theoretical Modeling of the o-Cresolphthalein Complexone Assay for Bone Calcium Resorption

by

Swetha Mohan

Master of Science in Bioengineering

University of California San Diego, 2020

Professor Robert L. Sah, Chair

O-cresolphthalein complexone (Ocpc) is a widely-used colorimetric indicator used to assess the Ca^{2+} concentration of biological and non-biological samples. To minimize interference by the ~ 0.8 - 1 mM Mg^{2+} present in culture media and biological samples, Ocpc has been used with 8-Hydroxyquinoline (8HQ) which preferentially binds to Mg^{2+} over Ca^{2+}. The Ocpc + 8HQ assay could be useful in *in-vitro* bioassays to estimate changes in Ca^{2+} concentration from the ~2 mM normally present in cell culture media. While several formulations of the Ocpc+8HQ assay have been suggested, their utility for such applications is unclear. The overall objectives of this project were (1) to develop a theoretical model of the Ocpc + 8HQ assay to assess Ca^{2+} release, and (2) to validate and apply this model to media in a bone resorption assay. Such a model can provide a quantitative understanding of how the different molecules of the assay system interact and contribute to the final output signal (OD). Models of increasing complexity were developed, ranging from 1.1. Model I - the reaction between Ocpc and Ca^{2+} to form the colored complex Caocpc 1.2. Model II - including interactions with 8HQ and 1.3. Model III - including interactions with Mg^{2+}. Next, the model was 2.1. Validated by comparing the linear region slopes of the

predicted and experimental calibration curves, and then 2.2. Applied to a bone resorption scenario by computing the sensitivity and specificity of the assay using relevant cell culture and bone resorption assay parameters. These theoretical models contribute to understanding the effect of the different complexes formed on the output signal. The results indicate the utility and limitations of an Ocpc + 8HQ assay for analysing Ca^{2+} from bioassays in culture medium. The modeling approach may be useful for other assays with target and interferent molecules.

CHAPTER 1 - INTRODUCTION

1.1 *In Vitro Bone* Resorption Assays

Osteoclasts are multinucleated and the only cells capable of bone resorption. Their differentiation is majorly regulated by macrophage colony-stimulating factor (MCS-F), RANK ligand (RANKL), and osteoprotegerin (OPG) [1-3]. Bone demineralization by osteoclasts usually involves the acidification of the extracellular microenvironment followed by degradation of organic components by enzymes [1]. The resorbing area under the ruffled border of osteoclasts is acidic, which favours dissolution of bone minerals [4]. They actively secrete lysosomal proteases into the resorption lacuna along with H^+ and Cl^- [5]. The osteoclast is a key target for characterizing and understanding disease models as well as developing drugs for resorptive bone diseases [6-11]. When there is an imbalance between resorption and formation of bone, the bone homeostasis is affected. Increased resorption increases risk of fractures. Such conditions are prevalent in bone disorders such as osteoporosis, hyperparathyroidism, renal osteodystrophy, Paget's disease and metastatic bone disease [11]. Osteoporosis is a metabolic disease that occurs due to an imbalance in skeletal turnover so that bone resorption exceeds the bone formation [12]. The mechanism of osteoclastogenesis and bone resorption by osteoclast is illustrated in **Figure 1.1**.

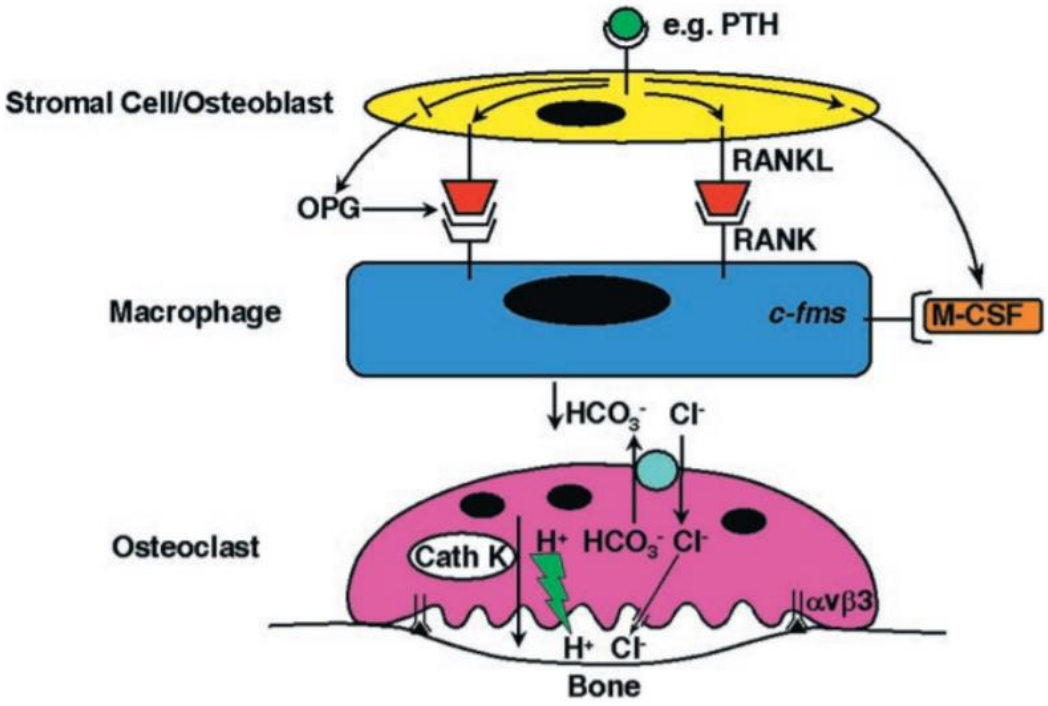

Figure 1.1: Mechanisms of osteoclastogenesis and osteoclastic bone resorption [1]

To study such mechanisms of the osteoclasts in order to understand diseases, several *in vitro* studies analyse factors affecting overall numbers of osteoclasts, osteoclast activation and differentiation that are key to regulating bone loss. *In vitro* studies have become important to characterize the factors that influence bone metabolism especially in disease conditions [10, 13-15]. In typical *in-vitro* resorption assays, the osteoclasts form pits and trails that are considered hallmarks of the osteoclastic activity. These assays are performed as either pure cultures or in coculture with other cell types such as osteoblasts along with a substrate for resorption typically like bone, dentin, HA substrates etc. The osteoclastic behavior can be extrapolated from such in-vitro experiments that help characterize the behavior as well as help build models for bone related diseases [7-9, 16]. These results are then used to develop several antiresorptive therapies against the excessive bone loss that tend to occur in numerous skeletal disorders [17].

Assessing the size of the pit and the number of pits formed by the osteoclasts are usually used as a measure of the resorptive capabilities of the osteoclast. The pits that are

formed are typically analyzed using light microscopic images and other 2D imaging techniques [6, 7, 16, 18, 19]. These techniques help estimate the area of resorption by osteoclasts and do not accurately capture the gradual 3D resorption process by the osteoclasts.

1.2 Extracellular Calcium and Bone Resorption

Osteoclasts used for *in-vitro* bone resorption assays are exposed to high levels of extracellular calcium due to the bone resorption. Through the progression of the resorption process Ca^{2+} is released into the micro-environment and gets accumulated. This extracellular Ca^{2+} has been shown to inhibit osteoclastic activity in a dose-dependent manner by transducing an increase in cytosolic Ca^{2+} concentrations [20, 21], and has been proposed as a negative-feedback mechanism for osteoclastic activity. Similar to parathyroid hormone (PTH)-secreting cells, a specialised surface receptor that detects changes in ambient Ca^{2+} concentration is believed to be responsible for this induction of Ca^{2+} signal across the cell membrane. A similar alteration of cytosolic Ca^{2+} concentration and inhibition of resorption upon exposure to other divalent ions such as Mg^{2+} and Ba^{2+} suggests that Ca^{2+} independently plays a role in extracellular regulation of and intracellular messaging in an osteoclast [22]. A significant change in resorption was noted at an ambient divalent ion concentration of 20 mM. Such changes in the cytosolic Ca^{2+} concentration also result in cell retraction [23] and reduction in secretion of osteoclastic enzymes such as TRAP [22], in addition to the inhibition of resorption.

High extracellular Ca^{2+} (~ 20 mM) at the start of a resorption experiment inhibits bone resorption by preventing the adhesion of osteoclasts to the bone slice. However, this inhibition is minimal when the spike in extracellular Ca^{2+} happens at a later time point after the start of the experiment [24]. At lower extracellular Ca^{2+} concentrations (~ 10 mM), osteoclast apoptosis has been proposed as a mechanism for calcium-induced inhibition of apoptosis [25]. Even an extracellular Ca^{2+} concentration of ~ 1.8 mM, roughly equal to the Ca^{2+} concentration of medium

+ serum, at the start of a bone resorption assay can result in ~ 20% of the cells becoming apoptotic after 72 hours.

Typical cell culture media has a background Ca^{2+} concentration of ~1.5 - 1.8 mM [17, 24] and that of serum is ~3-4 mM [26, 27]. For *in vitro* bone resorption assays, serum of 10% is widely used and hence, the final background Ca^{2+} concentration for such cell culture media is ~ 2 mM. Osteoclasts based on their origin resorb at different rates. Individual osteoclastic volumetric resorption rates range from 1,000-30,000 μm^3/(cell•day) [28]. Cortical bone, which is widely used as a substrate for *in vitro* bone resorption assays have ~25% of their dry weight to be Ca^{2+}. As the bone gets resorbed, the Ca^{2+} gets released into the microenvironment. In cases of in vitro assays, Ca^{2+} gets accumulated in the microenvironment until media is replaced. Such assays are typically conducted in a way that does not affect the cells or the resorption process. In that case, the Ca^{2+} shift from the basal concentration will be very small and a sensitive assay is required to measure these small changes.

1.4 Colorimetric Estimation of Ca^{2+}

O-cresolphthalein complexone is a widely used indicator of Ca^{2+} in both biological and non-biological samples. It is a triphenylmethane based chelating ligand that has two iminodiacetic acid functional groups. It reacts with alkaline earth metals and forms a deep purple color. At an alkaline pH the complex (H_6L) exists as H_2L^{4-} [29]. The structure of the Ocpc complex is shown in Figure 1.1

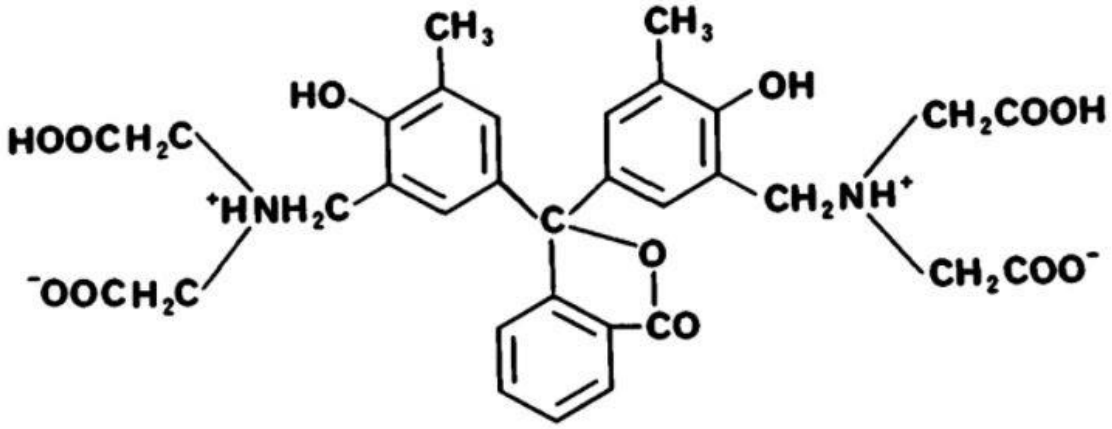

Figure 1.2: Structure of Ocpc [30]

In the initial stages of the assay development and usage, automated spectrophotometric procedures were described to estimate calcium in serum and urine [31]. These showed the direct application of such assay to biological samples [32]. Due to the interference by magnesium present in biological samples, the assays were then developed to also include a chelating molecule 8 Hydroxyquinoline [32-35]. 8 Hydroxyquinoline (C9H7NO) is a chelating molecule that can bind to divalent metal ions [36]. This molecule is known to preferentially bind to magnesium over calcium and hence, the effect of magnesium interference was observed to be masked in such systems [37].

Based on these developments, manual spectrophotometric methods were developed to test smaller batches of samples [33]. There have been different iterations of the assay over the years based on the different applications involved. Based on its application for biological samples like blood serum, since a major portion of the Ca^{2+} will be bound to proteins. Different assay's use different methods to isolate the Ca^{2+} ions from the proteins. Calcium oxalate has been decomposed using heat and the released calcium is estimated using the Ocpc reagent [38]. Another method used deproteinization buffers to precipitate the protein and estimate the calcium

amount [33] Even though the assay is widely used, the chemistry behind it was not extensively investigated. Especially the chemistry behind the cross reaction between the different components added and the effect of different concentrations of the species were unclear. Understanding how the input species react is essential to predict the output behavior of the assay.

All these different methods used a wide range of acids, buffers and bases and each assay is calibrated specifically based on the application at hand. These vary the final pH of the assay system while maintaining it between 10-12 for the reaction to occur. Even though the affinity of calcium ions to Ocpc is higher, since 8HQ can react to divalent cations, there is always some reaction between Ca^{2+} and 8HQ to form complexes that reduce the sensitivity. Similarly, the affinity of Mg^{2+} molecules to 8HQ is higher, but as mentioned earlier, they react to Ocpc. Mg^{2+} and Ocpc reactions are masked by 8HQ, but the cross reaction between Ca^{2+} and 8HQ will still be prevalent. The ligand strength of Ca^{2+} seems to be highest ~ pH 11 [33] and even small changes in pH is observed to have an effect on the ligand strength and hence alter the output signal.

Diethylamine used to be the most widely used base for this reaction to maintain the alkaline pH for it to occur. Since the cresolphthalein complexone was colored even in the absence of Ca^{2+} ions producing a high blank, 2-amino 2-methyl 1-propanol started being used to provide a more stable reaction assay system that overcomes the disadvantages like toxicity, volatility etc [39].

The effect of the different concentrations of species on the final output was unclear and hence, analysing the effect of each complex formed on the final output signal would help plan experiments with higher sensitivity and specificity to the target Ca^{2+}.

CHAPTER 2 - Theoretical Modeling of the Ocpc for Bone Calcium Resorption

2.1 ABSTRACT

Background: O-cresolphthalein complexone (Ocpc) is a widely-used colorimetric indicator used to assess Ca^{2+} concentration of biological samples. To minimize interference by the ~ 0.8 - 1 mM Mg^{2+} present in culture media and biological samples, Ocpc has been used with 8-Hydroxyquinoline (8HQ), which preferentially binds Mg^{2+} over Ca^{2+}. The Ocpc+8HQ assay can be useful to estimate changes in Ca^{2+} concentration above the ~2 mM normally present in cell culture media. While several formulations of the Ocpc+8HQ assay have been suggested, their utility for such applications is unclear.

Aims and approach: The overall objectives were to (1) develop a theoretical model of the Ocpc + 8HQ assay to assess Ca^{2+} release, and (2) to validate and apply this model to media in a bone resorption assay. Models of increasing complexity were developed starting with (1.1) the reaction between Ocpc and Ca^{2+} to form the colored complex Caocpc, extended (1.2) to include interactions with 8HQ, and finally, (1.3) include interactions with Mg^{2+}. Next, (2.1) the validity of the final model was assessed by comparing the linear region slopes of the predicted and experimental calibration curves and then, 2.2. applied to a bone resorption scenario by computing the sensitivity, specificity, and linear range of the assay using relevant cell culture and bone resorption assay parameters.

Results: (1) The effect of the different non-dimensional parameters on the concentration of Caocpc and the linearity of the calibration curve was ascertained. (1.1) When $\boldsymbol{\alpha} < 1$, i.e the concentration of total Ca^{2+} present in the system < concentration of total Ocpc, the assay output corresponded to the linear range. b) Increase in λ i.e the amount of 8HQ present in the system decreased the sensitivity of the curve and c) increase in $\boldsymbol{\eta}$ i.e Mg^{2+} present in the system

decreased the linear range in the absence of 8HQ and had no effect on the same in the presence of an appropriate amount of 8HQ. 2) The slopes of the linear regime of the predicted and experimental calibration curves were ~94% similar for the same input concentrations. For typical resorption assay parameters for a cortical bone in a 96 well plate, Ocpc of ~0.06 mM and a 8HQ of ~1 mM were appropriate for quantifying resorption-dependent Ca^{2+} increases after 1:80 dilution with a specificity of ~100% to 0.025 mM Ca^{2+} over 0.0125 mM Mg^{2+}.

Discussion: These theoretical models contribute to understanding the effect of the different complexes formed on the output signal. The results indicate the utility and limitations of an Ocpc+8HQ assay for analyzing Ca^{2+} from bioassays in culture medium. The modelling approach may be useful for other assays with target and interferent molecules.

2.2. INTRODUCTION

In vitro bone resorption assays typically quantify pit formation by cells seeded on target substrates by light microscopy [6, 7, 18, 19]. Osteoclasts (OCs) resorb hydroxyapatite (HA) mineral by localized H^+ secretion to acidify and enlarge resorption lacunae [40, 41]. The *in vitro* assay of osteoclast resorption has helped identify the role of key molecules, such as RANKL ligand (RANKL) and macrophage colony-stimulating factor (MCS-F) that regulate OC resorption [1-3]. Such functional regulation is important for elucidating mechanisms of bone related diseases like osteoporosis, hyperparathyroidism, renal osteodystrophy, and metastatic bone disease [6-11]. The area of the substrate perforated by such cells is typically estimated by transmitted light microscopy imaging and 2-dimensional image analysis [6, 7, 18, 19]. However, such analysis does not fully reflect the gradual and 3-dimensional nature of the resorption process. The release of calcium into the culture media may be a useful index of OC resorption of bone mineral.

The increased levels of extracellular Ca^{2+} during OC resorption *in vitro* may also regulate OCs in a physiologically-relevant manner [20, 24]. Typical media used in bone resorption assays

include DMEM, Alpha MEM, and Medium 199, often also containing serum [17, 24]. The Ca^{2+} concentration of these defined media are 1.5 - 1.8 mM [17, 24] and that of serum is ~3 - 4 mM [27, 42]. Individual osteoclastic volumetric resorption rates range from 1,000-30,000 μm^3/(cell•day) [28]. Of the dry weight of cortical bone, ~25% is Ca^{2+} [43-45]. The increase in Ca^{2+} concentration *in vitro* causes a dose-dependent inhibition of bone resorption and stimulation of osteoclast apoptosis at ~20 mM [25]. Thus, being able to assess medium Ca^{2+} concentration is useful, whether the goal is to maintain basal levels or to assess its effects on OC function.

The O-cresolphthalein complexone (Ocpc) can be used to estimate Ca^{2+} in media and serum, but is liable to interference by Mg^{2+} ions [29, 33-35, 46]. Ocpc is a triphenylmethane-based chelating ligand that has two iminodiacetic acid functional groups. It is usually denoted by H_2L^{4-} to indicate the two hydrogen ions that are present and ionizable under alkaline conditions. It binds a number of alkaline earth metals (M) to form MHL^{2-} complexes that provide the characteristic deep purple color that has a peak in light absorption at 560-590 nm. However, Ocpc can also bind to the ~0.8 - 1 mM Mg^{2+} present in culture media. Ca^{2+} and Mg^{2+} have different binding affinities for Ocpc, and the molar absorptivity at 580 nm for CaOcpc ($\varepsilon_{580}^{CaOcpc}$) is ~3.5 times that of MgOcpc ($\varepsilon_{580}^{MgOcpc}$) [33].

The interference of Ca^{2+} binding Ocpc by Mg^{2+} can be blocked by the chelator 8 Hydroxyquinoline (8HQ) [32-35]. 8HQ can chelate and complex alkaline earth metal ions [36]. Although 8HQ preferentially binds Mg^{2+} over Ca^{2+} [37], its binding of Ca^{2+} can compete with binding to Ocpc and reduce the sensitivity of the CaOcpc assay. Typical Ocpc assays that estimate Ca^{2+} concentration in biological samples use Ocpc, 8HQ, and an alkaline (pH 10-12) buffer. However, the effects of varying Ocpc and 8HQ concentrations on assay sensitivity and specificity are unclear.

Thus, the use of Ocpc to assess calcium shifts in media would be enhanced by more detailed and quantitative understanding of how the different molecules of the assay system interact and contribute to the absorbance signal. The specific objectives of this study were (1) to develop a theoretical model of the Ocpc + 8HQ assay to assess Ca^{2+} release, and (2) to validate and apply this model to media in a bone resorption assay. Models of variable complexity were developed, ranging from (Model I, Section 2.3.1.1) the reaction between Ocpc and Ca^{2+} to form the colored complex CaOcpc, (Model II, Section 2.3.1.2) the reaction including interactions with 8HQ, and (Model III, Section 2.3.1.3) the reaction including 8HQ and Mg^{2+}. Next, the model was (Section 2.3.2) validated and calibrated by comparing the predicted and experimental linear regions. Finally, (Section 2.3.3) the sensitivity and specificity of the assay in a model of *in vitro* bone resorption was analyzed using relevant cell culture and bone resorption assay parameters.

2.3. MODELS

2.3.1 Assay Model

Theoretical models of increasing complexity were developed in terms of the target of interest i.e the concentration of $CaOcpc^{2-}$ complex formed. The reactants and product complexes were denoted using their short forms along with their respective charges for deriving the models. Equilibrium relationships between the reactants and product complexes for each aforementioned system, along with their mass conservation equations were used to derive an expression for [$CaOcpc^{2-}$] for models I and II. Due to the complex nature of model III, analytical solutions were not possible. Numerical methods were used to calculate the concentration of $CaOcpc^{2-}$. The developed models were used to analyze the effect of Ca^{2+}, Mg^{2+}, $Ocpc^{4-}$ and 8HQ concentrations on the concentration of the colored complex of interest, $CaOcpc^{2-}$, that contributes to the output OD. The findings were used to determine the applicability of the assay to quantify calcium concentration shifts in bone resorption studies (**Section 2.3.3**)

Table 2.1. List of assay model parameters and variables

Variable / Parameter	Units	Description
$[8HQ_T]$, $[8HQ]$	mM	total and equilibrium concentrations of 8HQ
α		ratio of total concentrations of Ca^{2+} and $Ocpc^{4-}$
β		normalized equilibrium constant of Ca-Ocpc reaction with total $Ocpc^{4-}$ concentration
γ		$Caocpc^{2-}$ concentration at equilibrium normalized with total $Ocpc^{4-}$ concentration
λ		product of the equilibrium constant for the calcium-8HQ reaction and the square of input 8HQ concentration
ε_{CaOcpc}	$mM^{-1}cm^{-1}$	Molar absorptivity for $CaOcpc^{2-}$
ε_{MgOcpc}	$mM^{-1}cm^{-1}$	Molar absorptivity for $MgOcpc^{2-}$
$[Ca8HQ_2]$	mM	equilibrium concentration of $Ca8HQ_2$ complex
$[Ca_T^{2+}]$, $[Ca^{2+}]$,	mM	total and equilibrium concentrations of Ca^{2+}
$[CaOcpc^{2-}]$	mM	equilibrium concentration of $CaOcpc^{2-}$ complex
$[Mg_T^{2+}]$, $[Mg^{2+}]$	mM	total and equilibrium concentrations of Mg^{2+}
$[Mg8HQ_2]$	mM	equilibrium concentration of $Mg8HQ_2$ complex
$[MgOcpc^{2-}]$	mM	equilibrium concentration of $MgOcpc^{2-}$ complex
$[Ocpc_T^{4-}]$, $[Ocpc^{4-}]$	mM	total and equilibrium concentrations of $Ocpc^{4-}$
K_{CaOcpc}	mM^{-1}	equilibrium constant for the calcium - Ocpc reaction
K_{Ca8HQ2}	mM^{-2}	equilibrium constant for the calcium - 8HQ reaction
K_{MgOcpc}	mM^{-1}	equilibrium constant for the magnesium - Ocpc reaction
K_{Mg8HQ2}	mM^{-2}	equilibrium constant for the magnesium - 8HQ reaction

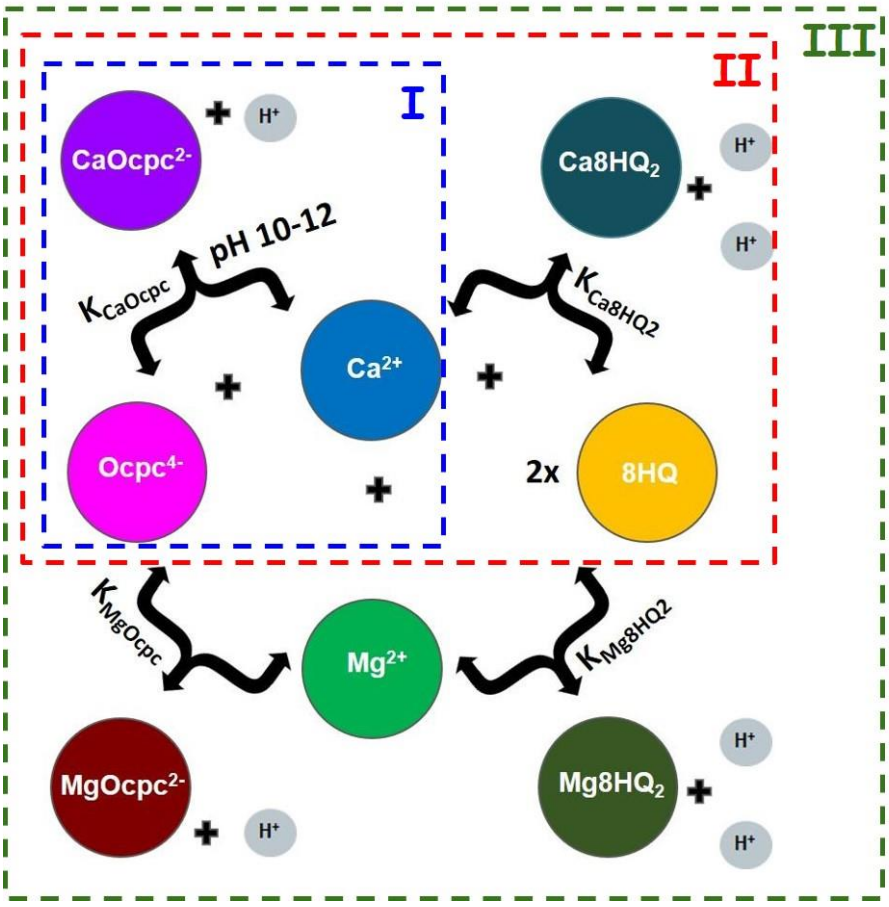

Figure 2.1: Schematic illustrating the reactants, product complexes and equilibrium constants for the developed models starting with (A) the simple reaction involving Ca^{2+} ions and Ocpc molecules reacting in a 1:1 ratio followed by (B) addition of 8HQ molecules and the resultant 2:1 complex formed with Ca^{2+} ions and finally, (C) the inclusion of Mg^{2+} ions and the respective 1:1 complex formed with $Ocpc^{4-}$ and 1:2 complex formed with 8HQ.

2.3.1.1 Model I with Ca^{2+} and $Ocpc^{4-}$

The concentration of the $CaOcpc^{2-}$ complex formed for model I, $[CaOcpc^{2-}]_I$, depends on the total input concentrations of Calcium ions $[Ca_T^{2+}]$, Ocpc molecules $[Ocpc_T^{4-}]$, the formation constant of the reaction, K_{CaOcpc}, and the alkaline pH of the assay system. Considering only the 1:1 ratio reaction between Ca^{2+} and $Ocpc^{4-}$ [30], the formation reaction for the target complex $CaOcpc^{2-}$ is given as,

$$Ca^{2+} + Ocpc^{4-} \underset{pH10-12}{\rightleftharpoons} CaOcpc^{2-} \quad (1)$$

The formation constant for this reaction (K_{CaOcpc}) relates the equilibrium concentrations of reactants and the products as,

$$K_{CaOcpc} = \frac{[CaOcpc^{2-}]_I}{[Ca^{2+}]_I[Ocpc^{4-}]_I} \tag{2}$$

$[Ca^{2+}]_I$ and $[Ocpc^{4-}]_I$ are the concentrations of the free calcium ions and free Ocpc ions, both at equilibrium. $1/K_{CaOcpc}$, which is also known as the dissociation constant of the complex, is equal to $[Ca^{2+}]_I$ when half the total $Ocpc^{4-}$ ($[Ocpc_T^{4-}]$) in a system is converted to $Caocpc^{2-}$ and the rest are present as free $Ocpc^{4-}$ i.e when $[CaOcpc^{2-}]_I = [Ocpc^{4-}]_I$.

At equilibrium, all the Ca^{2+} ions and $Ocpc^{4-}$ molecules exist freely or are bound to each other as the colored complex, $CaOcpc^{2-}$. Mass conservation for total Ca^{2+} and $Ocpc^{4-}$ in the system resulted in the following equations,

$$[Ca_T^{2+}] = [Ca^{2+}]_I + [CaOcpc^{2-}]_I \tag{3}$$

$$[Ocpc_T^{4-}] = [Ocpc^{4-}]_I + [CaOcpc^{2-}]_I \tag{4}$$

Non-dimensional parameters

$\boldsymbol{\alpha}$, $\boldsymbol{\beta}$ and $\boldsymbol{\gamma}_I$ denote the normalized versions of the input $[Ca_T^{2+}]$, the dissociation constant ($1/K_{CaOcpc}$) and the output $[CaOcpc^{2-}]$ respectively. All parameters were normalized with respect to $[Ocpc_T^{4-}]$.

$$\alpha = \frac{[Ca_T^{2+}]}{[Ocpc_T^{4-}]} \tag{5}$$

$$\beta = \frac{1}{K_{CaOcpc} * [Ocpc_T^{4-}]} \tag{6}$$

$$\gamma_I = \frac{[CaOcpc^{2-}]_I}{[Ocpc_T^{4-}]} \tag{7}$$

2.3.1.2 Model II with Ca^{2+}, $Ocpc^{4-}$ and 8HQ

In this system, the Ca^{2+} and 8HQ also react in a 1:2 ratio with low affinity to form $Ca8HQ_2$ complex alongside the formation of $CaOcpc^{2-}$ complex of interest [33],

$$Ca^{2+} + 2 * 8HQ \rightleftharpoons Ca8HQ_2 \tag{8}$$

The formation constant for $Ca8HQ_2$, K_{Ca8HQ2}, expressed in terms of the equilibrium concentrations of the reactant and the product species is given by,

$$K_{Ca8HQ_2} = \frac{[Ca8HQ_2]_{II}}{[Ca^{2+}]_{II}[8HQ]_{II}^2} \tag{9}$$

$[8HQ]_2$ is the concentration of free 8HQ molecules present at equilibrium in model II. $1/K_{Ca8HQ2,}$ which is also known as the dissociation constant of the complex, is equal to $[Ca^{2+}]_{II}$ when half the total 8HQ ($[8HQ_T]$) in a system is converted to $Ca8HQ_2$ and the rest are present as free 8HQ ie when $[Ca8HQ_2]_{II} = [8HQ]_{II}^2$. The formation constant for $CaOcpc^{2-}$ expressed in terms of equilibrium concentrations of reactants and products species for model II is given by

$$K_{CaOcpc} = \frac{[CaOcpc^{2-}]_{II}}{[Ca^{2+}]_{II}[Ocpc^{4-}]_{II}} \tag{10}$$

Conservation of mass for this system was given by

$$[Ca_T^{2+}] = [Ca^{2+}]_{II} + [CaOcpc^{2-}]_{II} + [Ca8HQ_2]_{II} \quad (11)$$

$$[Ocpc_T^{4-}] = [Ocpc^{4-}]_{II} + [CaOcpc^{2-}]_{II} \quad (12)$$

$$[8HQ_T] = [8HQ]_{II} + 2[Ca8HQ_2]_{II} \quad (13)$$

Model Assumptions

Since 8HQ has a low affinity for Ca^{2+}, K_{Ca8HQ2} will be very small and only a small fraction of the added $[8HQ_T]$ added gets converted to $Ca8HQ_2$. Moreover, high affinity of Ca^{2+} for $Ocpc^{4-}$ results in most of the free Ca^{2+} being sequestered by $Ocpc^{4-}$ molecules. Hence it's assumed that $[8HQ_T] >> [Ca8HQ_2]_{II}$.

Non-dimensional Equations

A new parameter λ that denoted the non-dimensionalized form of K_{Ca8HQ2} was introduced. The previously introduced parameters $\boldsymbol{\alpha}$, $\boldsymbol{\beta}$ and the normalized output $\boldsymbol{\gamma}_{II}$ were used in Model II.

$$\lambda = K_{Ca8HQ_2} * [8HQ_T]^2 \quad (14)$$

$$\gamma_{II} = \frac{[CaOcpc^{2-}]_{II}}{[Ocpc_T^{4-}]} \quad (15)$$

2.3.1.3 Model III with Ca^{2+}, $Ocpc^{4-}$, 8HQ, and Mg^{2+}

In this system, Mg^{2+} also reacts with $Ocpc^{4-}$ and 8HQ to form 1:1 and 2:1 complex, respectively.

$$Mg^{2+} + Ocpc^{4-} \rightleftharpoons MgOcpc^{2-} \tag{16}$$

$$Mg^{2+} + 2 * 8HQ \rightleftharpoons Mg8HQ_2 \tag{17}$$

The equilibrium expressions for the above reactions are given by

$$K_{Mg8HQ_2} = \frac{[Mg8HQ_2]_{III}}{[Mg^{2+}]_{III}[8HQ]^2_{III}} \tag{18}$$

$$K_{MgOcpc} = \frac{[MgOcpc^{2-}]_{III}}{[Mg^{2+}]_{III}[Ocpc^{4-}]_{III}} \tag{19}$$

Where K_{Mg8HQ2} and K_{MgOcpc} are the formation constants of the complexes $Mg8HQ_2$ and $MgOcpc^{2-}$ respectively. Conservation of mass for all the species in the system was given by

$$[Ca^{2+}_T] = [Ca^{2+}]_{III} + [CaOcpc^{2-}]_{III} + [Ca8HQ_2]_{III} \tag{20}$$

$$[Ocpc^{4-}_T] = [Ocpc^{4-}]_{III} + [CaOcpc^{2-}]_{III} + [MgOcpc^{2-}]_{III} \tag{21}$$

$$[8HQ_T] = [8HQ]_{III} + 2[Ca8HQ_2]_{III} + 2[Mg8HQ_2]_{III} \tag{22}$$

$$[Mg^{2+}_T] = [Mg^{2+}]_{III} + [MgOcpc^{2-}]_{III} + [Mg8HQ_2]_{III} \tag{23}$$

Non-dimensional parameter

A new parameter η was introduced that denotes the total concentration of Mg^{2+} in the system ($[Mg_T^{2+}]$), normalized with respect to $[Ocpc_T^{4-}]$.

$$\eta = \frac{[Mg_T^{2+}]}{[Ocpc_T^{4-}]} \tag{24}$$

The normalized output γ_{III} was used as a measure for model III

$$\gamma_{III} = \frac{[CaOcpc^{2-}]_{III}}{[Ocpc_T^{4-}]} \tag{25}$$

Model parameters

Concentrations of input values used for the models were from literature value ranges. $[Ca_T^{2+}]$ typically ranges from 0 mM (blank) to ~ 0.2 mM, and the lowest experimentally measured $[Ca_T^{2+}]$ concentration is ~0.005 mM [30]. $[Ocpc_T^{4-}]$ ranges from ~ 0.04 to 0.08 (**Table 2.2**)

Table 2.2. Low and high values of the input variables from literature and experimental data

Variable or parameter	units	Low value	High value	Reference
$[Ca_T^{2+}]$	mM	0	0.2	Corns, 1987
$[Ocpc_T]$	mM	0.04	0.08	Stern, 1957

Model I was used to determine the effect of increasing $\boldsymbol{\alpha}$ i.e increasing $[Ca_T^{2+}]$ in a system with constant $[Ocpc_T^{4-}]$ to mimic calibration curves. Twenty $\boldsymbol{\alpha}$ values between 0 to 1.67 corresponding to $[Ca_T^{2+}]$ values of 0 to 0.1 mM were chosen for this model. To determine the effect of different regimes of $\boldsymbol{\alpha}$, the ranges of interest were $\boldsymbol{\alpha} = 0$, $0<\boldsymbol{\alpha}<1$, $\boldsymbol{\alpha} \approx 1$ and $\boldsymbol{\alpha} > 1$ (**Table 2.3**). The same range of $\boldsymbol{\alpha}$ values were used for all 3 models (I, II and III). The equilibrium constant, $1/K_{CaOcpc,}$ at alkaline conditions has been determined to be 15.8×10^{-6} mM [47]. Since

in the calibration curve, $[Ocpc_T^{4-}]$ is the reagent that will be kept constant, the value of **β** for such calibration curve will be kept constant. The range of **β** values for the corresponding $[Ocpc_T^{4-}]$ range mentioned are between ~ 0.4×10^{-3} - 0.15×10^{-3}. For any typical $[Ocpc_T]$ value used in assay systems, **β** value was > 0 and << 1. An average $[Ocpc_T^{4-}]$ value of 0.06 mM was used for the models with the corresponding **β** value of 0.26×10^{-3}.

Table 2.3. Different ***α*** values used in the models

Case	$[Ca_T^{2+}]$	***α***
	mM	
1	0.000	0.000
2	0.005	0.083
3	0.050	0.833
4	0.100	1.677

A $1/K_{Ca8HQ2}$ value of 0.33 mM^2 was used in models II and III (unpublished data). Different λ values of 0, 3, 12 and 75 that correspond to $[8HQ_T]$ values of 0, 1, 2 and 5 mM respectively (**Table 2.4**) were used in model II.

Table 2.4. Different ***λ*** values used in the model and the corresponding $[8HQ_T]$

Case	$[8HQ_T]$	***λ***
	mM	
1	0	0
2	1	3
3	2	12
4	5	75

The values of $1/K_{MgOcpc}$ and $1/K_{Mg8HQ2}$ at a basic pH were determined to be 1.25×10^{-6} [47] and 0.16×10^{-6} mM [48] respectively. Based on background concentration of Mg^{2+} in culture media in final assay concentrations, the values η were chosen. The effect of η on the output was analysed by using three values of η - 0, 0.17 and 0.33 that correspond to $[Mg_T^{2+}]$ values of 0,

0.01 and 0.02 mM in the presence or absence of 5mM of [$8HQ_T$] (λ = 75 and 0, respectively) (**Table 2.5**).

Table 2.5. Different $\boldsymbol{\eta}$ and $\boldsymbol{\lambda}$ values used in model III

Case	$\boldsymbol{\lambda}$	[Mg_T^{2+}]	$\boldsymbol{\eta}$
		mM	
1	0	0.00	0.00
		0.01	0.17
		0.02	0.33
2	75	0.00	0.00
		0.01	0.17
		0.02	0.33

Analysis

The normalized $CaOcpc^{2-}$ concentration profile ($\boldsymbol{\gamma}$) for the three different models ($\boldsymbol{\gamma}_1$,$\boldsymbol{\gamma}_2$ and $\boldsymbol{\gamma}_3$) was plotted against different regimes of $\boldsymbol{\alpha}$ (**Table 2.3**) using MATLAB 2019a (The MathWorks, Inc., Natick, Massachusetts, United States). The input values mentioned in tables 2.3 and 2.4 were used to determine the $CaOcpc^{2-}$ concentration from the analytical solutions obtained for models I and II respectively. For numerical methods used in Model III, the MATLAB function Fsolve was used to calculate concentrations of $CaOcpc^{2-}$ using input values mentioned in **Table 2.5** This method internally uses the trust-region-dogleg algorithm to estimate the values of the unknowns based on the input values and initial guesses. The initial guesses provided were based on the relative concentrations and affinities of the different species. The concentration of complexes formed through bimolecular reactions were guessed to be equal to the concentration of the limiting reagent in that reaction. For competing reactions, such as the one between $Ocpc^{4-}$, Mg^{2+} and Ca^{2+}, the concentration of complex formed with greater affinity was guessed to be equal

to the concentration of the limiting reagent in the bimolecular reaction that produces it. The concentration of the complex formed with the competing, lower affinity molecule was guessed by comparing the concentration of said molecule with the concentration of ligand present after the high affinity reaction goes to completion.

2.3.2 Model validation

The validity of the model was tested by comparing experimental OD with predicted OD, determined by simulating the model under identical conditions as an experiment. The experimental data was obtained from a calibration curve assay performed in DMEM + 10% FBS. Increasing concentrations of Ca^{2+} std starting from 0 - 4 mM were prepared in media background Ca^{2+} concentration of 2.1 mM and a background Mg^{2+} concentration of 0.9 mM. $[8HQ_T]$ of 5.3 mM and $[Ocpc_T]$ of 0.06 mM were used for Ca^{2+} estimation. After 1:80 dilution of the standard samples to be assayed, $\boldsymbol{\alpha}$ values ranged from 0.44 to 1.1 and η values ranged from 0.19 to 0.11 in the final assay volume. $\boldsymbol{\varepsilon}_{CaOcpc}$ and $\boldsymbol{\varepsilon}_{MgOcpc}$ were determined to be 27 and 10.8 $mM^{-1}cm^{-1}$ respectively calculated from experimental data and assuming $\varepsilon_{CaOcpc} = 2.5*\varepsilon_{MgOcpc}$ [33]. The experimental and predicted calibration curves were plotted against $\boldsymbol{\alpha}$ and the slopes of the linear fits to $\boldsymbol{\alpha} < 1$ were compared using a two-tailed t-test.

2.3.3 Applicability to Bone Resorption Studies

A bone resorption model was developed to mimic the Ca^{2+} release in *in-vitro* bone resorption assay that uses DMEM + serum as media. The developed model was then used to estimate the change in output signal (OD) associated with resorption-dependent $[Ca^{2+}]$ shifts above the background Ca^{2+} for different media volumes. Lastly, the sensitivity and specificity of the $Ocpc^{4-}$ + 8HQ assay to quantify these shifts was estimated for different $[8HQ_T]$.

Bone Resorption Model

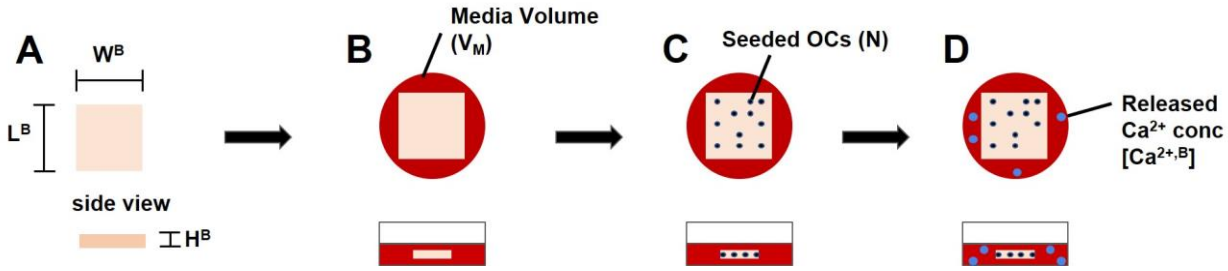

Figure 2.2: Schematic of the bone resorption model showing (A) a cortical bone tissue with length L^B, Width W^B and height H^B (B) placed in a 96 well plate with media volume of V_M seeded with (C) N osteoclasts and the respective (D) concentration of the released Ca^{2+} ions $[Ca^{2+,B}]$ into the environment from eroded bone.

The model defines a typical *in-vitro* bone resorption assay consisting of a small bone tissue (B) that could fit into the surface area and volume of a 96 well plate with osteoclasts (OCs) seeded on the bone. The OCs resorb the bone mineral and release Ca^{2+} ions of interest into the cell culture media + serum (**Figure 2.2**). The released Ca^{2+} accumulates in the cell culture media until the media gets replaced.

Table 2.6. List of bone resorption model parameters and variables

Variable / Parameter	Units	Description
ρ^B	g/cm^3	Density of cortical bone
Ω		Volume fraction of resorbed bone to media volume
$[Ca^{2+,B}]$	mM	Concentration of released Ca^{2+}
$[Ca_0^{2+}]$	mM	Concentration of Ca^{2+} in background source
F^B_{Ca}		Mass fraction of calcium present in cortical bone
L^B	cm	Length of bone substrate
$[Mg_0^{2+}]$	mM	Concentration of Mg^{2+} in background source
n	$\#/cm^2$	Seeding density of osteoclasts
N	#	Total number of osteoclasts
r^B_{BV}	#/(cell*day)	Volume fraction of resorbed bone per OC
r^B_B	g/(cell*day)	Rate of bone mass resorbed per OC
R^B_{Ca}	g/day	Rate of calcium mass resorbed per day
SA^B	cm^2	Surface area of bone substrate
T^B	cm	Thickness of bone substrate
V^B	cm^3	Volume of bone substrate
V_M	mL	Volume of culture media
W^B	cm	Width of bone substrate

Governing equations

The rate of bone resorbed (r^B_B) per cell per day for a bone substrate of length L^B, width W^B and thickness T^B is assumed to depend on the rate of bone volume fraction resorbed by single osteoclast in a day (r^B_{BV}) that is in relative to the total bone volume ($V^B = L^B*W^B*T^B$) and the density of the bone (ρ^B). It's given by the equation,

$$r_B^B = r_{BV}^B * V^B * \rho^B \tag{26}$$

The rate of calcium mass released per day (R^B_{Ca}), is estimated using the rate of bone resorbed (r^B), the mass fraction of calcium in cortical bone (F^B_{Ca}) and the total number of osteoclasts seeded on the bone slice (N),

$$R_{Ca}^B = r_B^B * F_{Ca}^B * N \tag{27}$$

where, the total number of osteoclasts seeded (N) is determined using the seeding density (n) and the surface area of the bone ($SA^B = L^B * W^B$)

$$N = n * SA^B \tag{28}$$

The concentration of calcium released [$Ca^{2+,B}$] can be calculated using the R^B_{Ca} for time T usually in a number of days along with the molecular weight of calcium (Ca_{MW}) and the media volume in which the resorption assay is carried out (V_M).

$$[Ca^{2+,B}] = \frac{\frac{(R_{Ca}^B * T)}{Ca_{MW}}}{V_M} \tag{29}$$

Bone resorption parameter **Ω** was introduced, that represented the ratio of the bone volume resorbed to the volume of the culture medium for T days. An expression for **Ω** was given by

$$\Omega = (r_{BV}^B * N * T) * \frac{V_B}{V_M} \tag{30}$$

Rearranging the equations to obtain an expression for [$Ca^{2+,B}$] in terms of **Ω** resulted in

$$[Ca^{2+,B}] = \frac{(\Omega * F_{Ca}^{B} * \rho^{B})}{Ca_{MW}} \quad (31)$$

Concentration of Ca^{2+} released into the media $[Ca^{2+,B}]$ is directly proportional to $\mathbf{\Omega}$ and can be increased or decreased by controlling parameters such as V_B, r^B_{BV}, N, T and V_M

Sensitivity and Specificity

The Ca^{2+} concentration of the assay solution is estimated at the time of replacement, and the increase in Ca^{2+} concentration above the basal concentration ($[Ca^{2+,B}]$) is attributed to osteoclast resorption. The assay volume chosen, V_M, must result in a quantifiable released Ca^{2+} concentration $[Ca^{2+,B}]$ shift above the background Ca^{2+} in media + serum $[Ca_0^{2+}]$. Quantifying $[Ca^{2+,B}]$ shifts also depends on the precision of the instrument used to measure OD, and to avoid saturation, the assay media is diluted before estimating calcium. The variability in the experimental OD, stemming from processes such as pipetting, can be interpreted as noise and the value V_M chosen should result in a high signal (OD due to $CaOcpc^{2-}$) to noise ratio. The signal by $[Ca^{2+,B}]$ can be calculated by,

$$\Delta OD = OD_T - OD_M \quad (32)$$

where, OD_T is the total OD measured on a given day for the resorption assay, OD_M is the signal generated by the background Ca^{2+} ($[Ca_0^{2+}]$) from culture media + serum, and ΔOD is the signal generated by the released Ca^{2+} $[Ca^{2+,B}]$ in a day.

The sensitivity of the assay to estimate $[Ca^{2+,B}]$ is assessed by describing the signal to noise ratio (SNR), where the variability due pipetting error as observed in experimental data is given by σ_{OD} i.e the noise.

$$SNR = \frac{\Delta OD}{\sigma_{OD}} \tag{33}$$

Considering the total signal contribution by the colored complexes as θ, Fractional contribution of $CaOcpc^{2-}$ (θ_{CaOcpc}) and $MgOcpc^{2-}$ (θ_{CaOcpc}) to the total output signal OD_T can be described as

$$\theta_{CaOcpc} = \frac{OD_{CaOcpc}}{OD_T} \tag{34}$$

$$\theta_{MgOcpc} = \frac{OD_{MgOcpc}}{OD_T} \tag{35}$$

where, the total signal as the sum of the fractional contribution is given by

$$\theta = \theta_{CaOcpc} + \theta_{MgOcpc} \tag{36}$$

Model Assumptions

It is assumed that the assay will take place in a 96 well plate for a cortical bone. No external stimuli were assumed to enhance resorption. The background Ca^{2+} ($[Ca_0^{2+}]$) and Mg^{2+} (Mg_0^{2+}) present in the system was assumed to be 2 mM and 1 mM respectively. The source of Mg^{2+} for this assay is only assumed to be from the culture media + serum as the Mg^{2+} content in bone is almost insignificant compared to the background $[Mg_0^{2+}]$ present. The assay media is assumed to be replaced every two days (N).

Model Parameters

The parameter values used in this model are from published values used in similar experiments from literature. The parameters used in this model include the bones surface area, volume, density and the calcium mass fraction present in the cortical bone, media volume for a 96 well plate, number of osteoclasts seeded and resorption rates of the bone by each osteoclast. The dimensions of the bone wafer used for such experiments vary with the type of well plate used and the application of it. Here, typical values used in similar experiments were chosen. The surface area of the bone (SA^B) used in the model was 0.25 cm^2 corresponding to the L^B and W^B value of 0.5 cm [49]. Volume of the bone V^B used was 0.005 cm^3 corresponding to a thickness of 0.02 cm [49]. Density of the bone (ρ^B) is in the range of 1.6 - 2 g/cm^3 [50]. The calcium mass fraction present in cortical bone (F^B_{Ca}) is estimated to be ~ 0.25 [43]. The media volume (V_M) in the 96 well plate for cell culture can range between 70 - 350 µL as the volume of media required to culture a monolayer of cells is ~200 $\mu L/cm^2$ [51] and this could also submerge bone wafers used of thicknesses up to 0.05 cm. The maximum volume a 96 well can hold is 360 µL and hence a culture volume limit of 350 µL was chosen for the model. The seeding density of OCs can have a range of values based on the application, typically ~1000 - 10000 $cells/cm^2$ [52, 53]. The sample dilution for this system was assumed to be 1:80.

Resorption rates used in the model depend on the rate of volume fraction of bone resorbed by each osteoclast per day relative to volume of bone (r^B_{BV}) which was calculated to be ~10^{-6} on an average for an osteoclast [28]. The value of reagent concentrations used were $[Ocpc_T]$ = 0.06 mM and $[8HQ_T]$ = 0, 1, 2 and 5 mM. A fixed value of 0.02 for σ_{OD} was used based on unpublished experimental results. Values used in the model are listed in (**Table 2.7**)

Table 2.7. Parameter values and ranges used in this model for the assay in 96 well plates

Parameter	Units	Values	References
SA^B	cm^2	0.25	Cheung, 1995
V^B	cm^3	0.005	Cheung, 1995
ρ^B	g/cm^3	1.6 - 2.0	Grimal, 2019
F^B_{Ca}		0.25	Quelch, 1983
V_M	µL	70 - 360	Gstraunthaler, 1999
N	$cells/cm^2$	10^3 - 10^4	Brinkmann, 2012 Vincent, 2008
r^B_{BV}	#/(cell*day)	10^{-6}	Kanehisa, 1988

Analysis

θ_{CaOcpc}, ΔOD and SNR were plotted against $\boldsymbol{\Omega}$ for different values of $[8HQ_T]$. $\boldsymbol{\Omega}$ values were calculated using the values in Table 2.5.

2.4 RESULTS

2.4.1.1 γ_1 linearly increased with α for $\alpha < 1$ and saturated for $\alpha > 1$

Upon solving the system of equations that make up Model I, an expression for γ_I was obtained in terms of α and β

$$\gamma_I(\alpha,\beta) = \frac{1}{2}\left(1 + \alpha + \beta \pm \sqrt{(1+\alpha+\beta)^2 - 4\alpha} \right) \tag{37}$$

The value of γ_I i.e. the concentration of complex $[CaOcpc^{2-}]_I$ formed should be zero when the value of α i.e. total calcium $[Ca_T^{2+}]$ is zero. The negative root satisfies this constraint and henceforth, the positive root was ignored. The simplified final equation obtained was

$$\gamma_I(\alpha,\beta) = \frac{1}{2}(\ 1+\alpha+\beta-\sqrt{(1+\alpha+\beta)^2-4\alpha}\ ) \tag{38}$$

The model for this system, described in terms of the non-dimensional constants $\boldsymbol{\alpha}$ and $\boldsymbol{\beta}$, showed that the normalized output $\boldsymbol{\gamma}_1$ linearly increases with increasing $\boldsymbol{\alpha}$ values and reaches a plateau for $\boldsymbol{\alpha}$ >1 shown in equations 38 - 44.

Case 1. When $\boldsymbol{\alpha}$ tends to 0 and 0 < $\boldsymbol{\beta}$ << 1

$$\lim_{\alpha\to 0}\gamma_I(\alpha,\beta) \approx 0 \tag{38}$$

Case 2. 0 < $\boldsymbol{\alpha}$ < 1 and 0 < $\boldsymbol{\beta}$ << 1

Taylor series expansion was used to expand the expression under the root about the point ($\boldsymbol{\alpha}$ = 0, $\boldsymbol{\beta}$ = 0)

$$\gamma_I(\alpha,\beta) \approx \frac{1}{2}(\ 1+\alpha+\beta-(1-\alpha+\beta+2\alpha\beta)\ ) \tag{39}$$

$$\gamma_I(\alpha,\beta) \approx \alpha(1-\beta) \tag{40}$$

Since $\boldsymbol{\beta}$ << 1, (1-$\boldsymbol{\beta}$) ≈ 1 and hence,

$$\gamma_I(\alpha,\beta) \approx \alpha \tag{41}$$

Lower $\boldsymbol{\alpha}$ values reflect a lower relative $[Ca_T^{2+}]$ concentration compared to the fixed $[Ocpc^{4-}]$ concentration, and hence, in this regime, $[Ca_T^{2+}]$ ends up being the limiting reagent. As $[Ca_T^{2+}]$ increases, a linear increase in $\boldsymbol{\gamma}_1$ (and the output $[CaOcpc^{2-}]_1$) was detected. However, this dependence is contingent upon the K_{CaOcpc} value being sufficiently high to keep $\boldsymbol{\beta} << 1$.

Case 3. $\boldsymbol{\alpha} \approx 1$ and $0 < \boldsymbol{\beta} << 1$

In this case, the output got simplified out to a fraction tending towards the value of 1 as $\boldsymbol{\alpha}$ value increases.

$$\gamma_I(\alpha, \beta) \approx \frac{(< 2)}{2} \tag{42}$$

Case 4. $\boldsymbol{\alpha} >> 1$ and $0 < \boldsymbol{\beta} << 1$

Since when $\boldsymbol{\alpha} >> 1$, $\boldsymbol{\beta}$ is insignificant compared to $\boldsymbol{\alpha}$ and hence,

$$\gamma_I(\alpha, \beta) \approx \frac{1}{2}(1 + \alpha - \sqrt{(\alpha - 1)^2}) \tag{43}$$

$$\gamma_I(\alpha, \beta) \approx 1 \tag{44}$$

At $\boldsymbol{\alpha} >> 1$, $[Ocpc_T^{4-}]$ added acts as a limiting factor and the curve saturates when

[$Ocpc_T^{4-}$] is fully utilized even if the [Ca_T^{2}] >> [$Ocpc_T^{4-}$]. Hence, [$CaOcpc^{2-}]_1$ ≈ [$Ocpc_T^{4-}$] at saturation.

The effect of the different $\boldsymbol{\alpha}$ values on the normalized output $\boldsymbol{\gamma}_1$ was shown by plotting $\boldsymbol{\gamma}_1$ vs a range of alpha values shown in Table 2.3. For a fixed [$Ocpc_T^{4-}$], as $\boldsymbol{\alpha}$ increases, $\boldsymbol{\gamma}_1$ also linearly increases and plateaus (**Figure 2.3.**). For an extended linear regime, which is the region of interest, the value of $\boldsymbol{\alpha}$ should be maintained < 1.

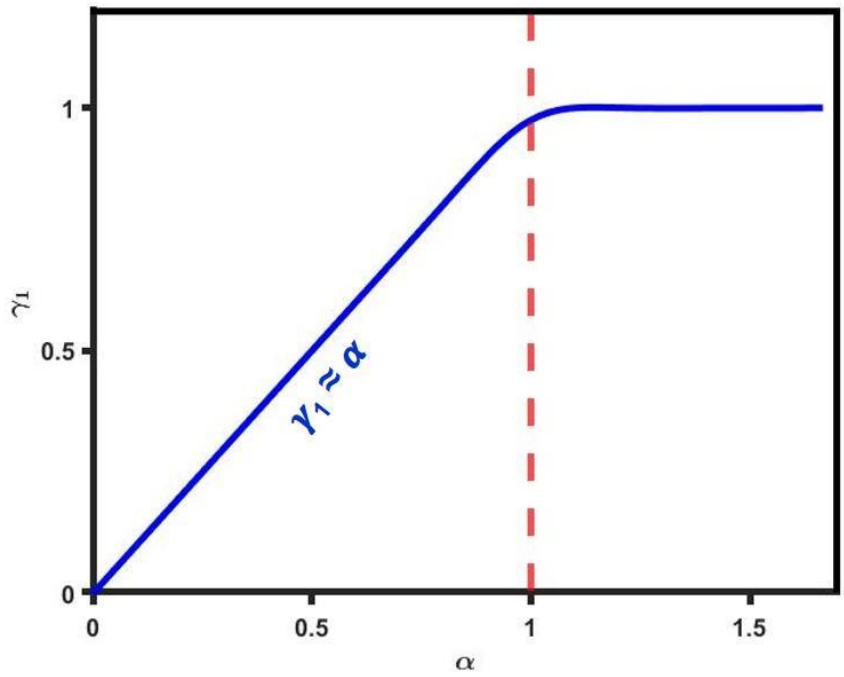

Figure 2.3: The normalized output $\boldsymbol{\gamma}_1$ plotted against $\boldsymbol{\alpha}$ illustrates the effect of varying $\boldsymbol{\alpha}$ on $\boldsymbol{\gamma}_1$. $\boldsymbol{\gamma}_1$ linearly increases with increase in [Ca_T^{2+}] when $\boldsymbol{\alpha}$ <1, plateaus when $\boldsymbol{\alpha}$ > 1 and transitions from linear to a plateau when $\boldsymbol{\alpha}$ ≈ 1.

2.4.1.2 Sensitivity of the assay decreased with increasing λ

Upon simplification of the mass balance and equilibrium relationships, an expression for $\boldsymbol{\gamma}_2$ was obtained in terms of $\boldsymbol{\alpha}$, **β** and **λ.**

$$\gamma_{II}(\alpha,\beta) \approx \frac{1}{2}\left(1+\alpha \pm \sqrt{1+\alpha(\alpha-2)+\beta^2(\lambda^2+2\lambda+1)+(\lambda+1)(2\alpha\beta+2\beta)} + \beta(\lambda+1) \right)$$

(45)

In the absence of 8HQ molecules, equation (45) should be the same as eq (37) from the previous model. Only the negative root satisfied this requirement,

$$\gamma_{II}(\alpha,\beta) \approx \frac{1}{2}\left(1+\alpha+\beta(\lambda+1) - \sqrt{1+\alpha(\alpha-2)+\beta^2(\lambda^2+2\lambda+1)+(\lambda+1)(2\alpha\beta+2\beta)}\ \right) \quad (46)$$

Curves with a higher λ value (and a higher [$8HQ_T$]) have a shorter linear regime (**Figure 2.4**). Increasing values of λ also resulted in reduced sensitivity due to the increased formation of $Ca8HQ_2$ complexes.

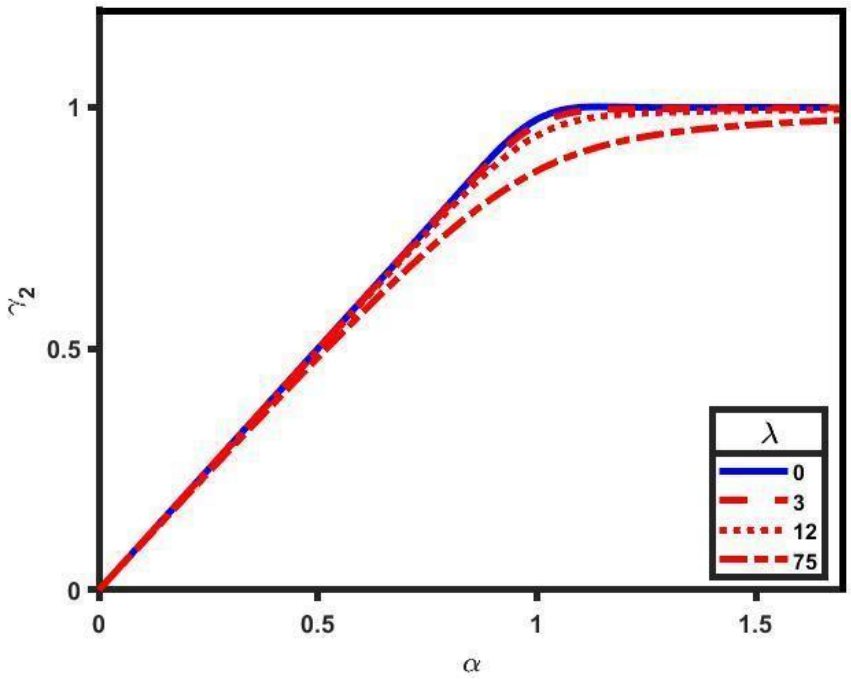

Figure 2.4: The normalized output γ_2 plotted against α illustrates the effect of varying λ on γ_2. As the [$8HQ_T$] added to the system increases, the sensitivity of the curve decreases due to the increasing formation of $Ca8HQ_2$ molecules.

2.4.1.3 Linear Range decreased with increasing values of η in the absence of 8HQ

Rearranging the system of nonlinear equations to get an expression for [$CaOcpc^{2-}$] resulted in a polynomial of degree > 5. According to the Abel-Ruffini Theorem, there is no analytical solution for polynomial equations of degree five or higher with arbitrary coefficients. Hence, numerical methods were used to solve this system of equations and obtain [$CaOcpc^{2-}$], [$MgOcpc^{2-}$], [$Ca8HQ_2$] and [$Mg8HQ_2$] for different input concentrations.

In the absence of 8HQ, the linear regime of the assay was shortened upon increasing the value of η as the Mg^{2+} ions compete with the Ca^{2+} ions for the free $Ocpc^{4-}$ ions present (**Figure 2.5 A**). As the value of [Mg_T^{2+}] increased, the [$Ocpc_T^{4-}$] available for Ca^{2+} in each system decreased and the curve saturated for a lower $\boldsymbol{\alpha}$ value. However, the use of 5 mM of 8HQ (λ = 75) masked the effect of Mg^{2+} by keeping the linear range intact for different values of [Mg_T^{2+}] present in the system while simultaneously reducing the sensitivity of the curve due to the formation of $Ca8HQ_2$ molecules (**Figure 2.5 B**).

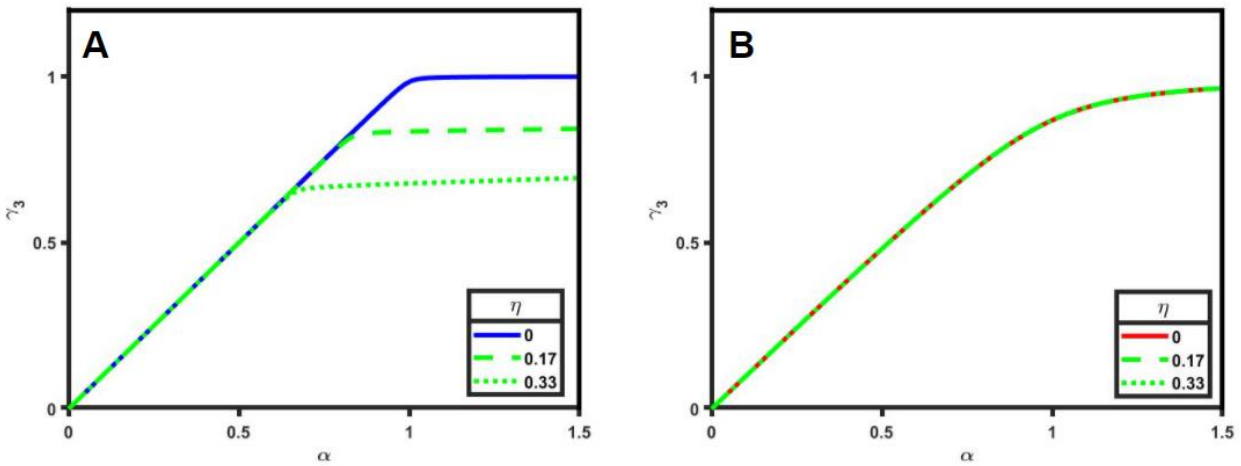

Figure 2.5: The normalized output $\boldsymbol{\gamma_3}$ plotted against $\boldsymbol{\alpha}$ illustrates the effect of varying η on $\boldsymbol{\gamma_3}$. As η increases with an increase in [Mg_T^{2+}] in the system, the linear range of the curves (A) gets shortened in the absence of [$8HQ_T$]. However, the 1 mM [$8HQ_T$] added to the system masks the (B) effect of Mg^{2+} but the sensitivity of the curve reduces due to the $Ca8HQ_2$ complexes formed.

2.4.2 The slopes of experimental and predicted curves are similar

The slopes of the linear regions of the predicted and experimental calibration curves were not significantly different (p = 0.70) (**Figure 2.6**.) with the slope of the experimental curve being ~94% similar to that of the predicted curve. Hence, the developed model accurately captures the behaviour of the linear regime of the assay.

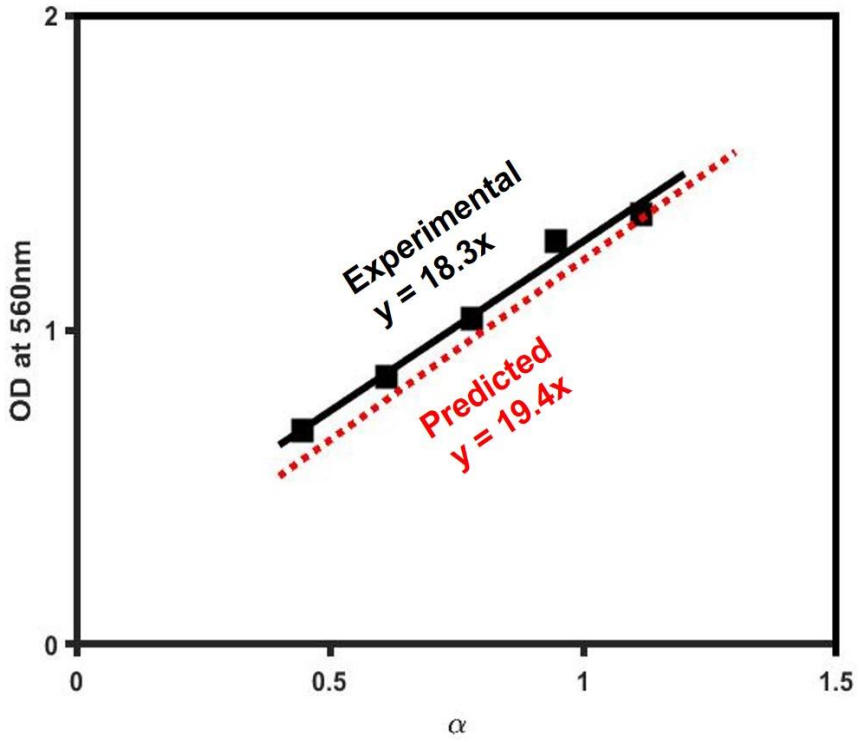

Figure 2.6: Experimental OD values at 560nm and the predicted OD values plotted against $\boldsymbol{\alpha}$ along with their regression lines for the same $[Ca_T^{2+}]$, $[Mg_T^{2+}]$, $[Ocpc_T^{4-}]$ and $[8HQ_T]$ values illustrate the similarities between the slopes

2.4.5 Assay sensitivity and specificity increased with increasing Ω and decreasing λ

Increasing **λ** values increased θ_{CaOcpc} by decreasing θ_{MgOcpc}, thereby increasing assay specificity to ~ 100% (**Figure 2.7 B.**). ΔOD and SNR increased with increasing values of **Ω** for a fixed amount of Mg^{2+} present in the system. ΔOD and SNR decreased with increasing λ, though the decrease was minimal for $\lambda \leq 12$ ($[8HQ_T] \leq 2mM$). The $\lambda = 0$ curve had a shorter linear regime compared to curves with $\lambda > 0$ due to the lack of availability of $Ocpc^{4-}$ for higher amounts of Ca^{2+}

present in the system. Hence, the addition of a $[8HQ_T]$ ~ 1 mM (λ = 3) completely masked the effect of 0.0125 mM of background Mg^{2+} for the $[Ca^{2+,B}]$ estimation (specificity ~ 100%) and increased the linear range of the assay without reducing assay sensitivity. (**Figure 2.7 A, B**)

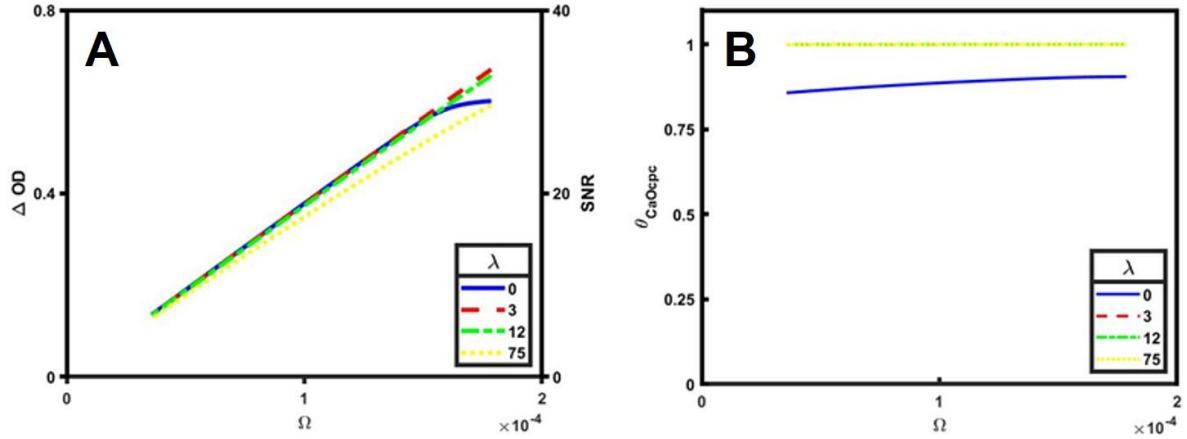

Figure 2.7: (A) ΔOD (left y axis), SNR (right y axis) and (B) Specificity of the assay when used for bone resorption assay, plotted for different $[8HQ_T]$ against **Ω**. $[8HQ_T]$ of 1 mM completely masks the non-specific absorbance caused by 0.0125 mM Mg^{2+} present in the media after 1:80 assay dilution. $[8HQ_T]$ values beyond this resulted in decreased sensitivity while getting ~100% specificity for Ca^{2+}.

2.5 DISCUSSION

This study described increasingly complex assay models that illustrate the effect of molecular interactions in an $Ocpc^{4-}$ + 8HQ assay for estimating Ca^{2+} and are applied to a bone resorption assay. The model solutions gave the target output concentration of $CaOcpc^{2-}$ for varying input concentrations of different species (Ca^{2+}, Mg^{2+}, $Ocpc^{4-}$, and 8HQ). The models were derived in terms of non-dimensional parameters and the effect of the different ranges of the parameters were tested on the output. The final model, including interactions between all species, predicted OD values that were similar to those determined experimentally. Further, the model was used to demonstrate the applicability of this assay to quantify Ca^{2+} released *in vitro* in cell-mediated bone resorption studies. A model was built to mimic the Ca^{2+} release in bone resorption assays and Ca^{2+} shifts were estimated for typical culture conditions. The specificity, sensitivity, and length of the linear regime of the $Ocpc^{4-}$ + 8HQ assay were determined while quantifying these shifts for different $[8HQ_T]$.

The ligands added, $Ocpc^{4-}$ and 8HQ, can interact and bind to the cations, Ca^{2+} and Mg^{2+}, in different ways. Here, it was assumed that $Ocpc^{4-}$ and 8HQ respectively only formed 1:1 and 2:1 complex with both Ca^{2+} and Mg^{2+}. However, complexes with other ratios have also been observed previously and their presence can alter the output OD. Further, the pH of the assay mixture was assumed to be maintained constant throughout and have no effect on the equilibrium constants used. Though a buffer is used to help maintain a constant basic pH, even a small change in pH has been found to noticeably alter ligand strengths of the species thereby affecting the output OD [33].

For the bone resorption model, other cations present in cell culture media, such as Fe^{3+}, K^+ and Na^+, were assumed to cause minimal/negligible interference. The effect of such cations

as they react with these ligands is unclear, however, the addition of 8HQ has been found to mask any interference caused by Iron (Beckman Coulter). It was also assumed that the resorption rate remains constant for the time interval considered. In practice, however, as the extracellular Ca^{2+} concentration increases with time due to resorption, a decrease in osteoclastic activity has been observed. All the osteoclasts added to the system were assumed to resorb the bone, while in experiments, some may stay inactive and not resorb.

The simple model (Model I, section 2.3.1.1) predicted that assay will be in the linear range when the value of $\alpha < 1$**.** The linear range is the region of interest to test samples with unknown Ca^{2+} concentrations. The saturation region corresponding to $\alpha > 1$ is the region to be avoided. The linear range of the $Ocpc^{4-}$ + 8HQ assay can be increased by 1) Increasing $[Ocpc_T^{4-}]$ and/or 2) Increasing the dilution factor of the test sample. The former results in the lengthening of the linear range without the sensitivity being compromised. The $[Ocpc_T^{4-}]$ used can be selected in a way that the resultant OD falls within the OD limits of the spectrophotometer. Increasing the dilution on the other hand, keeps the output signal within measurable limits albeit at the cost of reduced sensitivity.

The model that includes 8HQ (Model II, section 2.3.1.2) showed a decrease in assay sensitivity with increase in concentration of 8HQ added to the system. This was caused by an increase in the concentration of $Ca8HQ_2$ complex formed. The final model that includes all principal species i.e Ca^{2+},$Ocpc^{4-}$,8HQ and Mg^{2+} (Model III, section 2.3.1.3) showed the effect of Mg^{2+} on lowering the amount of $Ocpc^{4-}$ available for Ca^{2+} in the system to bind to in the absence of 8HQ molecules. In the presence of high amounts of 8HQ, almost all the Mg^{2+} present in the system were observed to be sequestered by the 8HQ molecules, thus eliminating the nonspecific absorbance. At the same time, the sensitivity of the curve was shown to be reduced due to the higher amounts of $Ca8HQ_2$ complexes formed. Hence, varying the concentration of different

species affected the linear range in different ways and experiments could be designed to minimize this loss in sensitivity.

The bone resorption model described helped predict the concentration of Ca^{2+} released from eroded bone above the background Ca^{2+} present in the system. Using the assay models developed, the signal (OD) corresponding to Ca^{2+} shifts in the system were determined. This helped analyze the sensitivity and specificity of the assay to measure the target Ca^{2+} shifts. Although, addition of 8HQ increases the specificity of the assay to target Ca^{2+} by ~100%, the sensitivity of the assay was lowered. Hence, lowering of sensitivity can also be minimized by using the smallest amounts of 8HQ that is enough to mask the amount of Mg^{2+} present in the system resulting in ~100% specificity (**Figure 2.7 A,B**). This can be determined by titrating different 8HQ concentrations in systems with different amounts of Mg^{2+} present to determine a suitable concentration of 8HQ to be used while maintaining assay sensitivity.

Several assumptions underlie the development of the assay model can be expanded upon to improve the model's prediction accuracy and usability. The inhibitory effect of extracellular Ca^{2+} on osteoclastic bone resorption can be mathematically factored in as a constraint when testing the applicability of the $Ocpc^{4-}$ + 8HQ assay for bone resorption studies. High extracellular Ca^{2+} concentration at the start of resorption reduces both the number of resorption pits formed per slice and the surface area per pit by reducing the number of osteoclasts that adhere to the bone slice [24]. Similarly, osteoclastic apoptosis caused by resorption dependent changes in $[Ca^{2+}]$ decreases the number of functioning cells (N). Modelling the number of osteoclasts as a function of the dynamic $[Ca^{2+}]$ can help inculcate these phenomena into our bone resorption model. The effect of the pH on both the assay system as well as the bone resorption process could be modeled by including the concentration of H^+ ions released into the system. Experiments can be performed to estimate Ca^{2+} from such bio-assays to validate the model and to build the model

further to improve the predictions. Since ~30-50% of the Ca^{2+} present in serum is bound to proteins [54], deproteinization methods help release bound Ca^{2+} and thus, detect the Ca^{2+} amounts present in the system more accurately. Such experiments could include estimation of Ca^{2+} at successive to time points to help predict the change in resorption rates over time. The effect of other media + serum components can be studied by using different media conditions with absence and presence of key components that could affect the measurement. These developed models could also be extended to build similar models for other systems with target and interfering molecules.

The study described in Chapter 2 of this paper is being prepared for submission for publication. Swetha, Mohan; Sah, Robert L. “Theoretical Modeling of the o-Cresolphthalein Complexone Assay for Bone Calcium Resorption”. The thesis author was the primary investigator and author of this material.

REFERENCES

1. Teitelbaum, S.L., *Osteoclasts: what do they do and how do they do it?* Am J Pathol, 2007. **170**(2): p. 427-35.

2. Dougall, W.C. and M. Chaisson, *The RANK/RANKL/OPG triad in cancer-induced bone diseases.* Cancer Metastasis Rev, 2006. **25**(4): p. 541-9.

3. Boyce, B.F. and L. Xing, *Functions of RANKL/RANK/OPG in bone modeling and remodeling.* Arch Biochem Biophys, 2008. **473**(2): p. 139-46.

4. Suda, T., I. Nakama, E. Jimi, and N. Takahashi, *Regulation of Osteoclast Function.* JBMR, 1997. **12**(6): p. 869-879.

5. Teitelbaum, S.L., *Osteoclasts and integrins.* Ann N Y Acad Sci, 2006. **1068**: p. 95-9.

6. Lees, R.L. and J.N. Heersche, *Macrophage colony stimulating factor increases bone resorption in dispersed osteoclast cultures by increasing osteoclast size.* J Bone Miner Res, 1999. **14**(6): p. 937-45.

7. Moon, S.J., I.E. Ahn, H. Jung, H. Yi, J. Kim, Y. Kim, S.K. Kwok, K.S. Park, J.K. Min, S.H. Park, H.Y. Kim, and J.H. Ju, *Temporal differential effects of proinflammatory cytokines on osteoclastogenesis.* Int J Mol Med, 2013. **31**(4): p. 769-77.

8. Sung, B., S. Prasad, V.R. Yadav, S.C. Gupta, S. Reuter, N. Yamamoto, A. Murakami, and B.B. Aggarwal, *RANKL signaling and osteoclastogenesis is negatively regulated by cardamonin.* PLoS One, 2013. **8**(5): p. e64118.

9. James, I.E., M.W. Lark, D. Zembryki, E.V. Lee-Rykaczewski, S.M. Hwang, T.A. Tomaszek, P. Belfiore, and M. Gowen, *Development and characterization of a human in vitro resorption assay: demonstration of utility using novel antiresorptive agents.* J Bone Miner Res, 1999. **14**(9): p. 1562-9.

10. Bradley, E.W. and M.J. Oursler, *Osteoclast culture and resorption assays.* Methods Mol Biol, 2008. **455**: p. 19-35.

11. Boyce, B.F., E. Rosenberg, A.E. de Papp, and L.T. Duong, *The osteoclast, bone remodelling and treatment ofmetabolic bone disease.* Eur J Clin Invest, 2012. **42**(12): p. 1332-1341.

12. Teitelbaum, S.L., *Osteoporosis and integrins.* J Clin Endocrinol Metab, 2005. **90**(4): p. 2466-8.

13. Husheem, M., J.K. Nyman, J. Vääräniemi, H.K. Vaananen, and T.A. Hentunen, *Characterization of circulating human osteoclast progenitors: development of in vitro resorption assay.* Calcif Tissue Int, 2005. **76**(3): p. 222-30.

14. Hsu, H., D.L. Lacey, C.R. Dunstan, I. Solovyev, A. Colombero, E. Timms, H.L. Tan, G. Elliott, M.J. Kelley, I. Sarosi, L. Wang, X.Z. Xia, R. Elliott, L. Chiu, T. Black, S. Scully, C. Capparelli, S. Morony, G. Shimamoto, M.B. Bass, and W.J. Boyle, *Tumor necrosis factor*

receptor family member RANK mediates osteoclast differentiation and activation induced by osteoprotegerin ligand. Proc Natl Acad Sci U S A, 1999. **96**(7): p. 3540-5.

15. Buchwald, Z.S., J.R. Kiesel, R. DiPaolo, M.S. Pagadala, and R. Aurora, *Osteoclast activated FoxP3+ CD8+ T-cells suppress bone resorption in vitro.* PLoS One, 2012. **7**(6): p. e38199.

16. Rumpler, M., T. Würger, P. Roschger, E. Zwettler, I. Sturmlechner, P. Altmann, P. Fratzl, M.J. Rogers, and K. Klaushofer, *Osteoclasts on bone and dentin in vitro: mechanism of trail formation and comparison of resorption behavior.* Calcif Tissue Int, 2013. **93**(6): p. 526-39.

17. Collin-Osdoby, P. and P. Osdoby, *RANKL-mediated osteoclast formation from murine RAW 264.7 cells.* Methods Mol Biol, 2012. **816**: p. 187-202.

18. Tamura, T., N. Takahashi, T. Akatsu, T. Sasaki, N. Udagawa, S. Tanaka, and T. Suda, *New resorption assay with mouse osteoclast-like multinucleated cells formed in vitro.* J Bone Miner Res, 1993. **8**(8): p. 953-60.

19. Merrild, D.M., D.C. Pirapaharan, C.M. Andreasen, P. Kjærsgaard-Andersen, A.M. Møller, M. Ding, J.M. Delaissé, and K. Søe, *Pit- and trench-forming osteoclasts: a distinction that matters.* Bone Res, 2015. **3**: p. 15032.

20. Zaidi, M., H.K. Datta, A. Patchell, B. Moonga, and I. MacIntyre, *'Calcium-activated' intracellular calcium elevation: a novel mechanism of osteoclast regulation.* Biochem Biophys Res Commun, 1989. **163**(3): p. 1461-5.

21. Malgaroli, A., J. Meldolesi, A.Z. Zallone, and A. Teti, *Control of cytosolic free calcium in rat and chicken osteoclasts. The role of extracellular calcium and calcitonin.* J Biol Chem, 1989. **264**(24): p. 14342-7.

22. Zaidi, M., J. Kerby, C.L.-H. Huang, A.S.M.T. Alam, H. Rathod, T.J. Chambers, and B.S. Moonga, *Divalent Cations Mimic the Inhibitory Effect of Extracellular Ionised Calcium on Bone Resorption by Isolated Rat Osteoclasts: Further Evidence for a "Calcium Receptor".* J Cell Physiol, 1991. **149**: p. 422-427.

23. Bax, B.E., V.S. Shankar, C.M. Bax, A.S. Alam, S. Zara, B.S. Moonga, M. Pazianas, C.L. Huang, and M. Zaidi, *Functional consequences of the interaction of Ni2+ with the osteoclast Ca2+ 'receptor'.* Exp Physiol, 1993. **78**(4): p. 517-29.

24. Hall, T.J., *A reappraisal of the effect of extracellular calcium on osteoclastic bone resorption.* Biochem Biophys Res Commun, 1994. **202**(1): p. 456-62.

25. Lorget, F., S. Kamel, R. Mentaverri, A. Wattel, M. Naassila, M. Maamer, and M. Brazier, *High extracellular calcium concentrations directly stimulate osteoclast apoptosis.* Biochem Biophys Res Commun, 2000. **268**(3): p. 899-903.

26. Blankenship, J.R. and J. Heitman, *Calcineurin Is Required for Candida albicans To Survive Calcium Stress in Serum.* Infect Immun, 2005. **73**(9): p. 5767-5774.

27. Branzoi, I.V., M. Iordoc, F. Branzoi, R. Vasilescu-Mirea, and G. Sbarcea, *Influence of diamond-like carbon coating on the corrosion resistance of the NITINOL shape memory alloy.* Surf Interface Anal, 2009. **42**(6-7): p. 502-509.

28. Kanehisa, J. and J.N. Heersche, *Osteoclastic bone resorption: in vitro analysis of the rate of resorption and migration of individual osteoclasts.* Bone, 1988. **9**(2): p. 73-9.

29. Paull, B., M. Macka, and P.R. Haddad, *Determination of calcium and magnesium in water samples by high-performance liquid chromatography on a graphitic stationary phase with a mobile phase containing o-cresolphthalein complexone.* J Chromatogr A, 1997. **789**: p. 329-337.

30. Corns, C.M. and C.J. Ludman, *Some observations on the nature of the calcium-cresolphthalein complexone reaction and its relevance to the clinical laboratory.* Ann Clin Biochem, 1987. **24**: p. 345-351.

31. Kessler, G. and M. Wolfman, *An Automated Procedure for the Simultaneous Determination of Calcium and Phosphorus.* Clin Chem, 1964. **10**: p. 686-703.

32. Gitelman, H.J., *An improved automated procedure for the determination of calcium in biological specimens.* Anal Biochem, 1967. **18**: p. 521-31.

33. Connerty, H.V. and A.R. Briggs, *Determination of serum calcium by means of orthocresolphthalein complexone.* Am J Clin Pathol, 1966. **45**(3): p. 290-6.

34. Baginski, E.S., S.S. Marie, W.L. Clark, and B. Zak, *Direct microdetermination of serum calcium.* Clin Chim Acta, 1973. **46**(1): p. 49-54.

35. Lorentz, K., *Improved determination of serum calcium with 2-cresolphthalein complexone.* Clin Chim Acta, 1982. **126**: p. 327-334.

36. Prachayasittikul, V., S. Prachayasittikul, S. Ruchirawat, and V. Prachayasittikul, *8-Hydroxyquinolines: a review of their metal chelating properties and medicinal applications.* Drug Des Devel Ther, 2013. **7**: p. 1157-78.

37. Shah, S., A.G. Dalecki, A.P. Malalasekera, C.L. Crawford, S.M. Michalek, O. Kutsch, and J. Sun, *8-Hydroxyquinolines Are Boosting Agents of Copper-Related Toxicity in Mycobacterium tuberculosis.* 2016. **60**(10): p. 5765-76.

38. Stern, J. and W.H. Lewis, *The colorimetric estimation of calcium in serum with ocresolphthalein complexone.* Clin Chim Acta, 1957. **2**(6): p. 576-80.

39. Moorehead, W.R. and H.G. Biggs, *2-Amino-2-methyl-1-propanol as the alkalizing agent in an improved continuous-flow cresolphthalein complexone procedure for calcium in serum.* Clin Chem, 1974. **20**(11): p. 1458-1460.

40. Blair, H.C., S.L. Teitelbaum, R. Ghiselli, and S. Gluck, *Osteoclastic bone resorption by a polarized vacuolar proton pump.* Science, 1989. **245**(4920): p. 855-7.

41. Väänänen, H.K. and T. Laitala-Leinonen, *Osteoclast lineage and function.* Arch Biochem Biophys, 2008. **473**(2): p. 132-8.

42. Blankenship, J.R., F.L. Wormley, M.K. Boyce, W.A. Schell, S.G. Filler, J.R. Perfect, and J. Heitman, *Calcineurin is essential for Candida albicans survival in serum and virulence.* Eukaryot Cell, 2003. **2**(3): p. 422-30.

43. Quelch, K.J., R.A. Melick, P.J. Bingham, and S.M. Mercuri, *Chemical composition of human bone.* Arch Oral Biol, 1983. **28**(8): p. 665-74.

44. Mitchell, H.H., T.S. Hamilton, F.R. Steggerda, and H.W. Bean, *The chemical composition of the adult human body and its bearing on the biochemistry of growth.* J Biol Chem, 1945. **158**: p. 625-637.

45. Forbes, R.M., A.R. Cooper, and H.H. Mitchell, *The composition of the adult human body as determined by chemical analysis.* J Biol Chem, 1953. **203**(1): p. 359-66.

46. Hu, W.W., Y.T. Hsu, Y.C. Cheng, C. Li, R.C. Ruaan, C.C. Chien, C.A. Chung, and C.W. Tsao, *Electrical stimulation to promote osteogenesis using conductive polypyrrole films.* Mater Sci Eng C Mater Biol Appl, 2014. **37**: p. 28-36.

47. Cheng, K.L., K. Ueno, and T. Imamura, *Handbook of Organic Analytical Reagents*. CRC Press.

48. Maley, L.E. and M.D. P., *The Relative Stability of Internal Metal Complexes. I. Complexes of 8-Hydroxyquinoline, Salicylaldehyde, and Acetylacetone.* Aust J Sci Res B, 1949. **2**(1): p. 92-110.

49. Cheung, R.C., C. Gray, A. Boyde, and S.J. Jones, *Effects of ethanol on bone cells in vitro resulting in increased resorption.* Bone, 1995. **16**(1): p. 143-7.

50. Grimal, Q. and P. Laugier, *Quantitative ultrasound assessment of cortical bone properties beyond bone mineral density.* IRBM, 2019. **40**(1): p. 16-24.

51. Gstraunthaler, G., T. Seppi, and W. Pfaller, *Impact of culture conditions, culture media volumes, and glucose content on metabolic properties of renal epithelial cell cultures. Are renal cells in tissue culture hypoxic?* Cell Physiol Biochem, 1999. **9**(3): p. 150-72.

52. Brinkmann, J., T. Hefti, F. Schlottig, N.D. Spencer, and H. Hall, *Response of osteoclasts to titanium surfaces with increasing surface roughness: an in vitro study.* Biointerphases, 2012. **7**(1-4): p. 34.

53. Vincent, C., M. Kogawa, D.M. Findlay, and G.J. Atkins, *The generation of osteoclasts from RAW 264.7 precursors in defined, serum-free conditions.* J Bone Miner Metab, 2009. **27**(1): p. 114-9.

54. Moore, E.W., *Ionized calcium in normal serum, ultrafiltrates, and whole blood determined by ion-exchange electrodes.* J Clin Invest, 1970. **49**(2): p. 318-34.